

By W. C. LINDSEY and T. O. ANDERSON

Summary. This paper is devoted to the problem of tracking data-transitions in digital communication systems by means of decision-directed phase-tracking loops. Such techniques are of interest because these methods provide the receiver with a knowledge of the time instants when the modulation may change states without using additional transmitter power. The results presented are useful in designing synchronizing circuitry for a wide variety of digital systems. One particular system mechanization plan is presented.

Introduction. Recently considerable interest has developed in the problem of tracking data-transitions in digital communication systems. The application of this technique is to provide the receiver with an accurate estimate of symbol synchronization, i.e., the instants in time when the modulation may change states. In so-called single-channel (Ref. 1) digital communication systems where symbol and subcarrier synchronization are derived from the recovered modulation such a method offers a saving in transmitter power over the so-called two-channel (Ref. 2) system where a separate timing signal is transmitted for synchronization purposes. This article presents an analysis of a particular type of symbol-tracking device. System mechanization techniques are also suggested. The results are useful in designing synchronizing circuitry for a wide variety of digital systems, e.g., block decoders and sequential decoders.

System Model. A block diagram of a digital data-transition tracking loop is depicted in Fig. 1. The tracking loop consists of two branches: an "In-Phase" branch, the upper half, and a "Mid-Phase" branch, the lower half. These two branch outputs, viz., $I(t_n)$ and $M(t_n)$, are fed into a phase detector, the loop multiplier, producing the signal $e(t_n)$ which is filtered by the loop filter $F(s)$. The output, say $v(t)$, of $F(s)$ is used to control the instantaneous frequency and phase of the voltage control oscillator (VCO). The VCO output is used to control a time generator which produces the time ticks t_n for sampling the output of the in-phase and mid-phase filters. The decision device accepts the output from the in-phase (IP) filter and announces "+1" if the input is greater than zero and "-1" if the input is less than zero. This information is fed into the transition detector whose outputs are either "+1", "-1", or "0". Since the transition "blue" depends on the input up until time t_n , whereas the mid-symbol integral depends only on times up to $t_n - T/2$, it is necessary to delay the mid-symbol integral by $T/2$ sec to give a number $M(t_n)$ to the loop. This effectively inserts the function $e^{-T/2}$ into the open loop transfer function; but, as we shall assume $\omega_L T \ll 1$, its effect on loop operation is negligible and is hence omitted in the analysis to follow. [ω_L is the loop bandwidth (Ref. 3)]. The transition value "+1" is assumed if the data sequence goes from plus to minus, i.e., a negative-going transition occurs. If no transition in the data takes place the output $I(t_n)$ is set to zero. The mid-phase (MP) filter is, in effect, the error channel of the loop and the algebraic sign of its output is switched in accordance with signal $I(t_n)$ to produce the so-called tracking loop S-curve. The input signal $x(t)$, which in practice is the output of a subcarrier tracking loop, is assumed to be the sum of a signal $s(t)$ plus additive white Gaus-

sian noise $n(t)$. In what follows we present an analysis which enables one to design such a loop, determine the range in data rate and signal-to-noise ratio in the loop bandwidth w_L , etc. for which the loop will provide the necessary timing accuracy required for symbol synchronization. Loop performance depends upon three parameters, viz., the energy per symbol E_s , noise spectral density N_0 , and the ratio δ_s of the symbol rate $R_s = \frac{1}{T_s}$ to the loop bandwidth w_L as a measure of performance.

System Analysis and Design Trends. It is assumed that the input signal $x(t)$ consists of a sequences of pulses of time duration T and random amplitude $\pm A$ where the probability of $+A$ equals the probability of $-A$, and that the additive noise $n(t)$ is white and Gaussian with single-sided spectral density of N_0 watts/hertz. Thus

$$x(t) = \sum_n b_n u(t - nT - \epsilon) + n(t) \quad (1)$$

where $u(t) = 1$ if $0 \leq t \leq T$ and $u(t) = 0$ elsewhere. In (1) ϵ is the random epoch to be estimated and $b_n = \pm A$ with $p(+A) = p(-A) = \frac{1}{2}$.

The procedure which we use to analyze loop behavior is to develop an equivalent model of the loop from which the nonlinear theory of tracking loops, viz., the Fokker-Planck apparatus (Ref. 3), may be used to specify loop performance. This involves two computations: (1) determination of loop S-curve on the average as a function of the normalized offset $\lambda = \tau/T$ from the lock point $\tau = \epsilon - \hat{\epsilon}$, and (2) determination of the spectral density about the origin of the equivalent noise as a function of the normalized offset λ . We shall refer to this spectral density as $S(\omega, \lambda)$ and the S-curve as $g(\lambda)$. We assume that the noise which disturbs the loop is white and Gaussian with a double-sided spectral density of $S(0, \lambda)$ watts/hertz. For all practical purposes, then, the equivalent transition tracking loop of Fig. 1 may be replaced by the mathematically equivalent loop illustrated in Fig. 2. In Fig. 2 the spectral density of $n_\lambda(t_n)$ is denoted by $S(0, \lambda)$ and K is the product of the VCO gain constant and the gain of the loop's phase detector. Obviously, $S(0, \lambda)$ is monotonically increasing in λ , since the further away from the lock point ($\lambda = 0$) the more noise one has to contend within $I(t_n)$. This is due to the fact that more errors are made in the "In-Phase" branch which, in effect, injects more noise into the multiplier of Fig. 1.

If little data degradation can be tolerated, then extreme accuracy is required in establishing symbol synchronization. Thus, the value of $S(0, \lambda)$ is essentially the noise spectral density seen by the loop at $\lambda = 0$, viz., $S(0, 0)$. If one assumes that the in-phase filter and the mid-phase filter are perfect integrators with integration time T seconds, then it may be shown that the S-curve is expressed by

$$g(\lambda) = AT\lambda [1 - 2P_{E_t}(\lambda)] ; \quad |\lambda| \leq \frac{1}{2} \quad (2)$$

where $P_{E_t}(\lambda)$ is the probability of detecting a transition incorrectly, viz.,

$$P_{E_t}(\lambda) = \frac{1}{\sqrt{2\pi}} \int_A^\infty \exp(-x^2/2) dx \quad (3)$$

where $A = 2R_s(1 - 2|\lambda|)$ and $R_s = A^2 T / N_0$. Figure 3 illustrates the S-curve $g(\lambda)$ for various values of R_s . It is seen that, for large R_s , the curves are linear while for smaller R_s the curves are highly dependent upon R_s . Also, it may be shown that

$$S(0,0) = \frac{N_0 T}{4} \left[1 + \frac{R_s}{2} \left\{ \frac{1}{\sqrt{\pi}} \exp(-R_s) + R_s (1 - P_{E_t}(0)) \right\}^2 \right] \quad (4)$$

$$= \frac{N_0 T}{4} h$$

in which h represents the bracketed quantity. Obviously, as R_s approaches infinity $S(0,0) = N_0 T / 4$ as it should, i.e., h approaches unity.

The stochastic differential equation which relates the pertinent parameters to the loop model in Fig. 2 may be written as (assuming zero static timing error)

$$\dot{\lambda} = KF(p)[A g(\lambda) + n_\lambda(t)] \quad (5)$$

where $\lambda = \tau/T = (\epsilon - \hat{\epsilon})/T$. Since solving stochastic differential equations is meaningful only in the probabilistic sense we seek to determine the probability distribution $p(\lambda)$ by the Fokker-Planck method (Ref. 3). Without belaboring the details of the derivation, we have that

$$p(\lambda) = N \exp \left[- \frac{2R_s \delta_s}{h} \int_{-\frac{1}{2}}^{\lambda} x [1 - 2P_{E_t}(x)] dx \right]; \quad |\lambda| \leq \frac{1}{2} \quad (6)$$

where N is chosen such that $p(\lambda)$ has unit area and $\delta_s = 1/Tw_L = R_s/w_L$. It is clear from Eq. 6 that for small $P_{E_t}(x)$, i.e., large R_s that $p(\lambda)$ becomes Gaussian with variance, as determined from Eq. 6, of

$$\sigma_\lambda^2 = \frac{h}{2R_s \delta_s} = \frac{hN_0 w_L}{2A^2} \quad (7)$$

In the linear region of operation the variance of the normalized timing error is proportional to the signal-to-noise ratio in the loop bandwidth w_L . From (6) it can be seen that $p(\lambda)$ becomes uniformly distributed as $\delta_s R_s = A^2 / N_0 w_L$ approaches zero. The variance of the normalized timing error, given by

$$\sigma_\lambda^2 = 2 \int_0^{\frac{1}{2}} \lambda^2 p(\lambda) d\lambda \quad (8)$$

has been obtained using numerical integration; the results are illustrated in Fig. 4 for a wide range of design parameters.

As an alternate mechanization of the tracking loop, it is possible to improve loop performance by reducing the noise variance $S(0,\tau)$ at the expense of changing the S-curve. This may be accomplished by integrating in the mid-phase channel only over a portion of the symbol time, say w sec-

onds. In this case, it may be shown that the S-curve is given by (see Fig. 5)

$$g(\lambda) = \begin{cases} AT\lambda[1 - 2P_{E_t}(\lambda)] & ; \quad 0 \leq \lambda \leq w/2T \\ Aw[1 - 2P_{E_t}(\lambda)] & ; \quad w/2T \leq \lambda \leq w/T \end{cases} \quad (9)$$

and the corresponding values of the noise spectra density about $w = 0$ is given by

$$s(0,0) = \frac{N_0 wh'}{4} \quad (10)$$

Thus, it would appear that the noise $S(0,0)$ may be made arbitrarily small by allowing w to approach zero; however, the problem of symbol slipping around the lock point begins to degrade the loops tracking capability. It would appear, then, that there exists a "best" w for a given mean time to first symbol slip.

In the linear region of loop operation the variance of the normalized loop jitter is thus given by

$$\sigma_\lambda^2(w) = \frac{wh'}{2R_s} \cdot w_L \quad (11)$$

Comparing this with the situation $w = T$ (i.e., integration over the full symbol time in the error channel) we have

$$\frac{\sigma_\lambda^2(w)}{\sigma_\lambda^2} = \frac{h'}{h} \cdot \frac{w}{T} \approx \frac{w}{T} \quad (12)$$

in the linear region. So the improvement in normalized jitter is approximately w/T . If $w = T/2$ then there is an approximate 3 db improvement, i.e., $w/T = \frac{1}{2}$. As before one may write the probability density $p(\lambda)$ using Fokker-Planck methods, however, we shall not study the details here.

System Mechanization. In this section we discuss one particular implementation of the symbol synchronizer analyzed in the previous section. This implementation, illustrated in Fig. 6, includes several novel features intended to provide for a wide range of symbol rates R_s , viz., 10 to 250 kilobits per second. This wide range in R_s is made possible and is simplified by implementing the tracking loop in the hybrid digital-analog domain.

For large symbol rates, multiplexing between two separate integrators in the IP branch is performed so that one may reset one integrator while employing the other integrator. The outputs of the IP filters serve as inputs to two high-speed tracking converters¹ (HSTC). Multiplexing between the two HSTC's of the IP branch is then performed in the digital domain; thus, eliminating any degradation due to manipulation of the analog signal.

¹ Manufactured by Canoga Electronics Corporation, Chastworth, California.

In the previous section it was demonstrated analytically that best tracking performance is obtained by integrating over a portion of the symbol time, see the timing chart illustrated in Fig. 7. Integration over a portion of a symbol time in the MP filter leaves ample time for resetting of the integrator; thus, no multiplexing in the MP branch is required. The mechanization of this branch consists of an integrate and dump circuit followed by hard limiter.

The loop filter (see Fig. 6) is implemented digitally as a perfect integrator. The transfer function $F(s)$ assumes the form

$$F(s) = K_1 + \frac{K_2}{s} \quad (13)$$

\uparrow first-order component \uparrow second-order component

so that operational problems due to false lock, static phase-error, etc., are minimized. Both components are implemented individually in the digital domain and added in the analog domain. The first-order component is a positive or a negative number entered in a register by an accepted sample from the MP branch. The second-order component is the running sum of accepted samples of the same branch. These samples are counted in a up/down counter. Attached to the outputs of the up/down counter and hold register are digital-to-analog converters (DAC). The outputs of these two DAC's are added at the input of an operational amplifier (OP) whose output is used as an error signal to control the instantaneous phase and frequency of the VCO.

The bandwidth is controlled by varying the gain in each component of the digital filter, i.e., the gain K_1 is implemented by setting the register to various gain levels while the gain K_2 is implemented by tapping the appropriate stage at the input to the up/down counter. This counter also controls the decade selection of the VCO frequency. The VCO output is used to trigger the timing generator.

Initial acquisition of symbol sync may be achieved by a lowering of the gains K_1 and K_2 (widens the loop bandwidth) and inserting an acquisition voltage into the VCO which causes its frequency to vary slowly with respect to the incoming symbol rate. When symbol lock is achieved the loop bandwidth is narrowed so as to give better tracking performance. Alternatively, if a computer is available for loop filter processing, it can be programmed for automatic acquisition. In this case the VCO is replaced by a frequency synthesizer and the loop bandwidth and instantaneous frequency of the synthesizer are controlled via the computer.

Description of Operation. Integration is performed over a symbol time by the IP filter and over a portion of a symbol time for the MP filter. If two consecutive samples of the IP output differ in sign, a symbol transition is assumed to have occurred. The sample from the MP filter is used to form the correction voltage for the VCO. If two consecutive samples of IP filter are of the same sign, no transition is assumed to have occurred and the MP filter sample is discarded. The accepted samples are processed in the digital filter and the result is used as the correction voltage. To provide flexibility in detail timing for the integrators and high speed tracking converters, the VCO frequency is selected to be several times the symbol rate. This frequency is counted down by the timing generator in Fig. 6.

Finally, the correction voltage is normalized as follows: A zero to one and one to zero data transition occurring at the same out-of-phase position would result in correction voltages of opposite polarity. This discrepancy is corrected by multiplying the correction voltage by the sign of one branch of the MP channel. The detection of a transition as well as this multiplication are performed in the digital domain by means of the mod 2 circuits illustrated. Delay registers excluded from the diagram must be included so that two consecutive samples from the in-phase branch, and the sample from the mid-phase branch will be available for processing at the same time. The output registers of the two in-phase high-speed tracking converters are de-multiplexed to derive the final output of the bit synchronizer.

A system mechanization such as described above is presently being implemented at the Jet Propulsion Laboratory. It is intended to be used in conjunction with a sequential decoder in support of the Pioneer D spacecraft to be launched in August 1968.

References

1. Lindsey, W. C., "Optimal Design of One-Way and Two-Way Coherent Communication Links", IEEE Transactions on Communication Technology, Vol. COM-14, No. 4, August, 1966.
2. Lindsey, W. C., "Determination of Modulation Indexes and Design of Two-Channel Coherent Communication Systems", IEEE Transactions on Communication Technology, Vol. COM-15, No. 2, pp. 229-237, April, 1967.
3. Lindsey, W. C. and R. C. Tausworthe, "A Survey of Phase-Locked Loop Theory". To be published in the book entitled, Recent Advances in Space Communication, McGraw-Hill Book Company, edited by A. V. Balakrishnan.

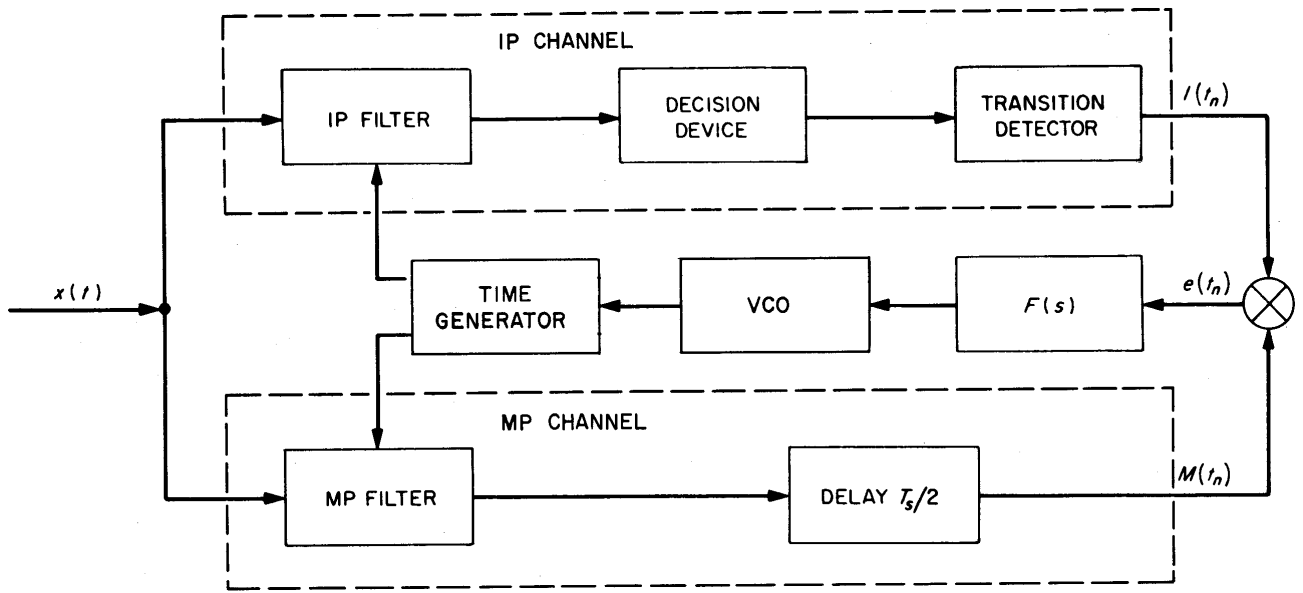


Fig. 1. DATA-TRANSITION TRACKING LOOP

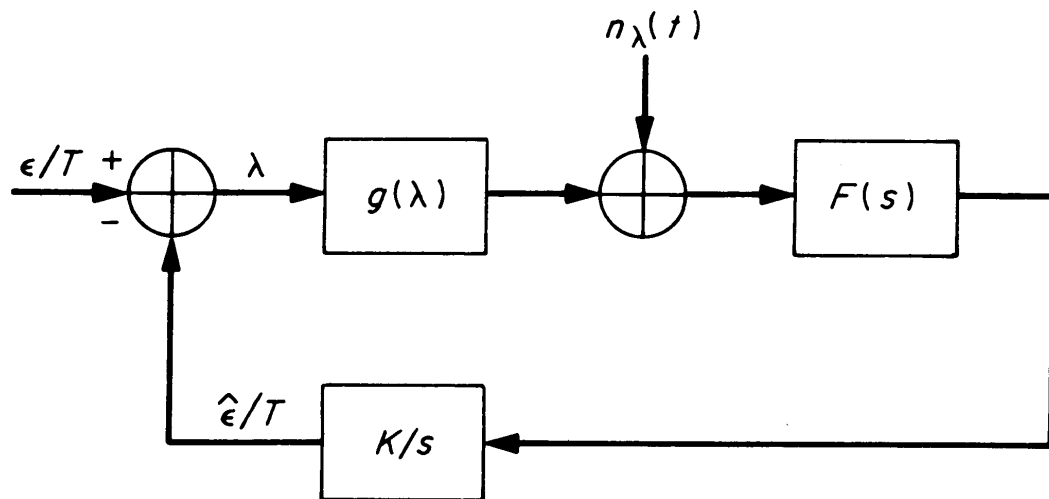


FIG. 2. EQUIVALENT DATA-TRANSITION TRACKING LOOP MODEL

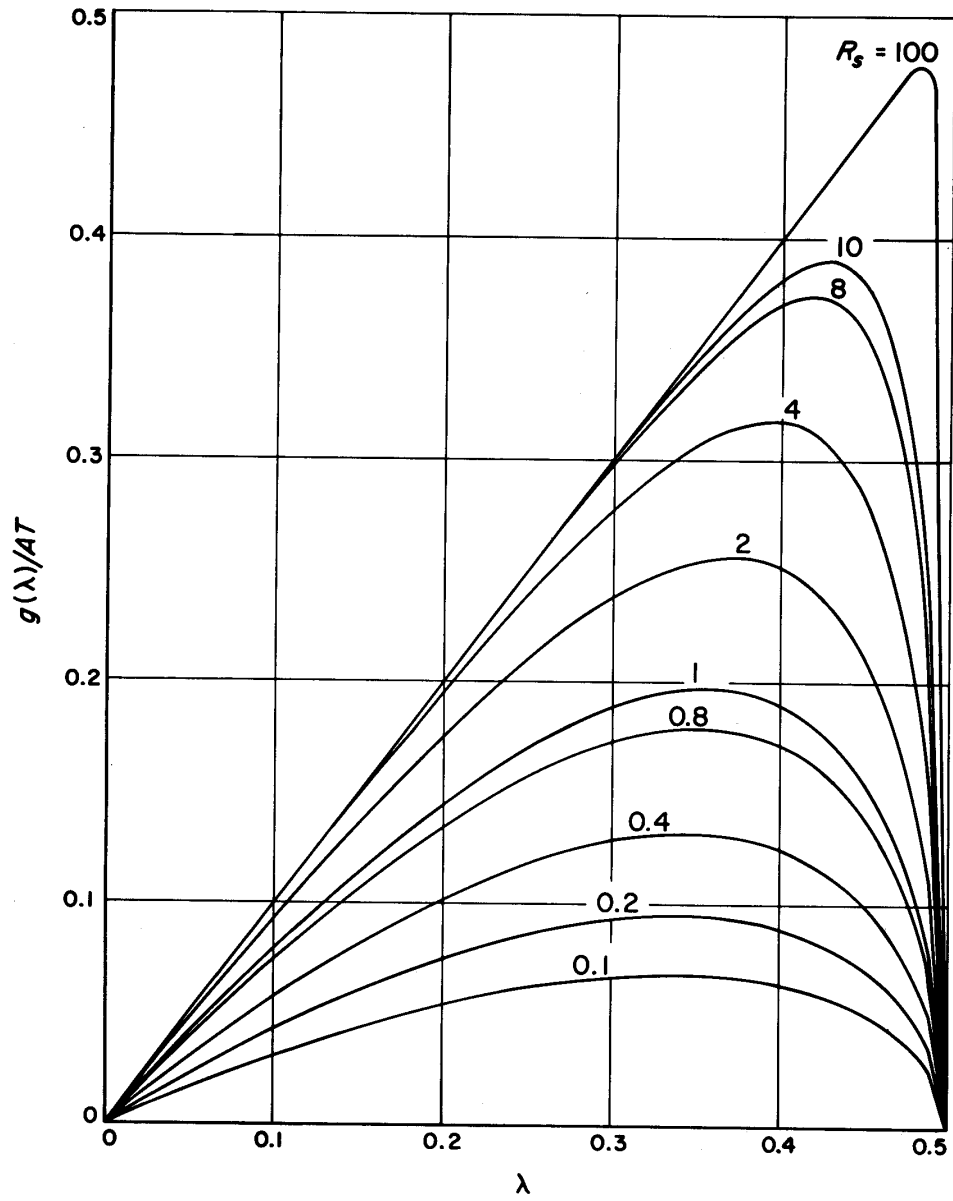


FIG. 3. THE FUNCTION $g(\lambda)/AT$ vs λ FOR VARIOUS R

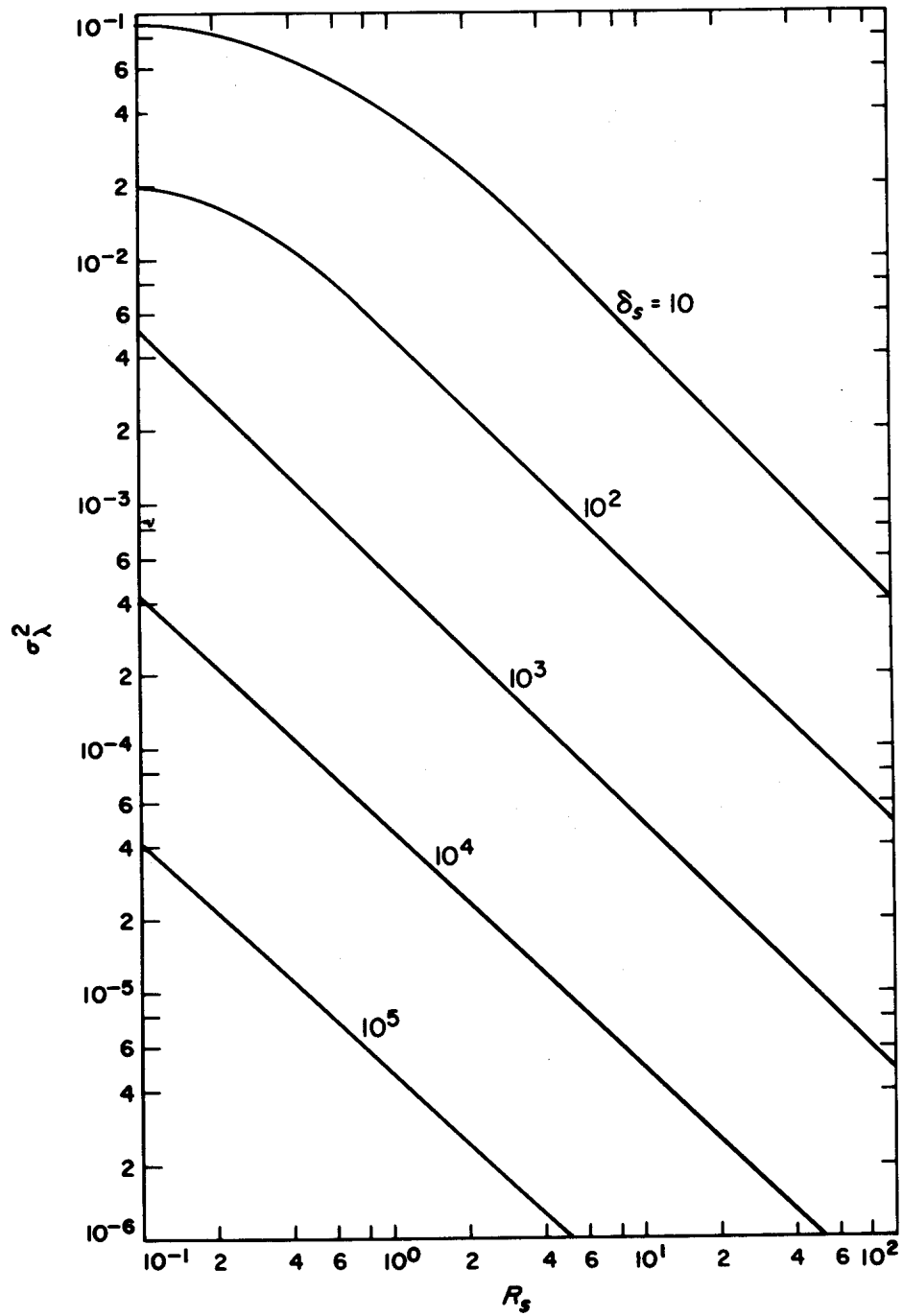


FIG. 4. VARIANCE σ_λ^2 OF THE NORMALIZED JITTER vs R_s FOR VARIOUS VALUES OF δ_s

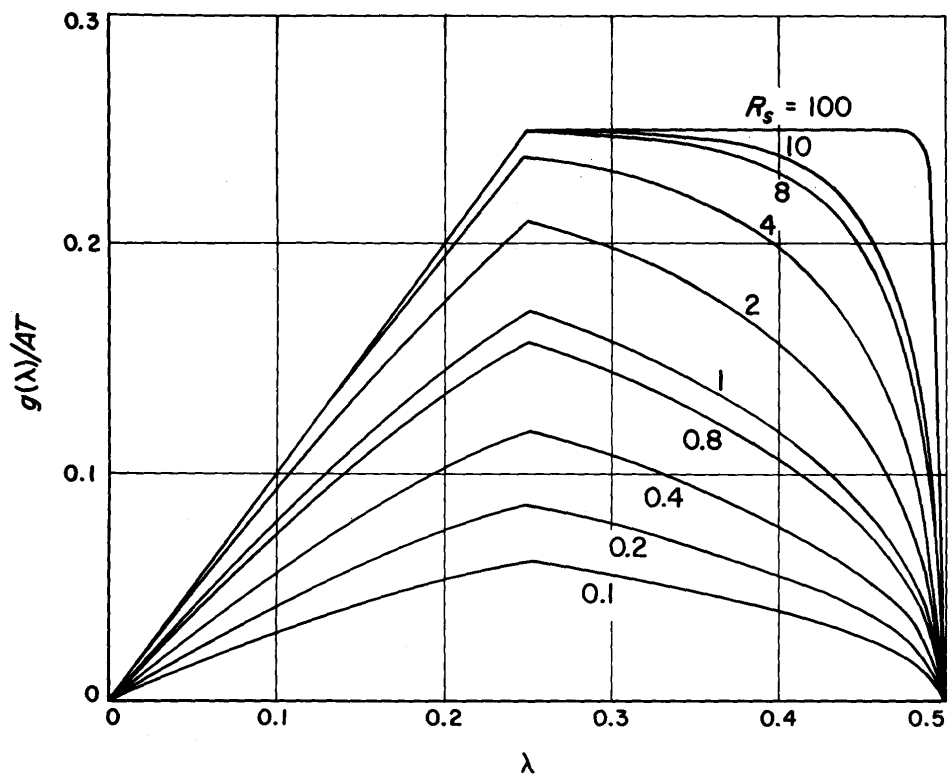


FIG. 5. THE FUNCTION $g(\lambda)/AT$ vs λ FOR VARIOUS R_s WITH $w = T/2$

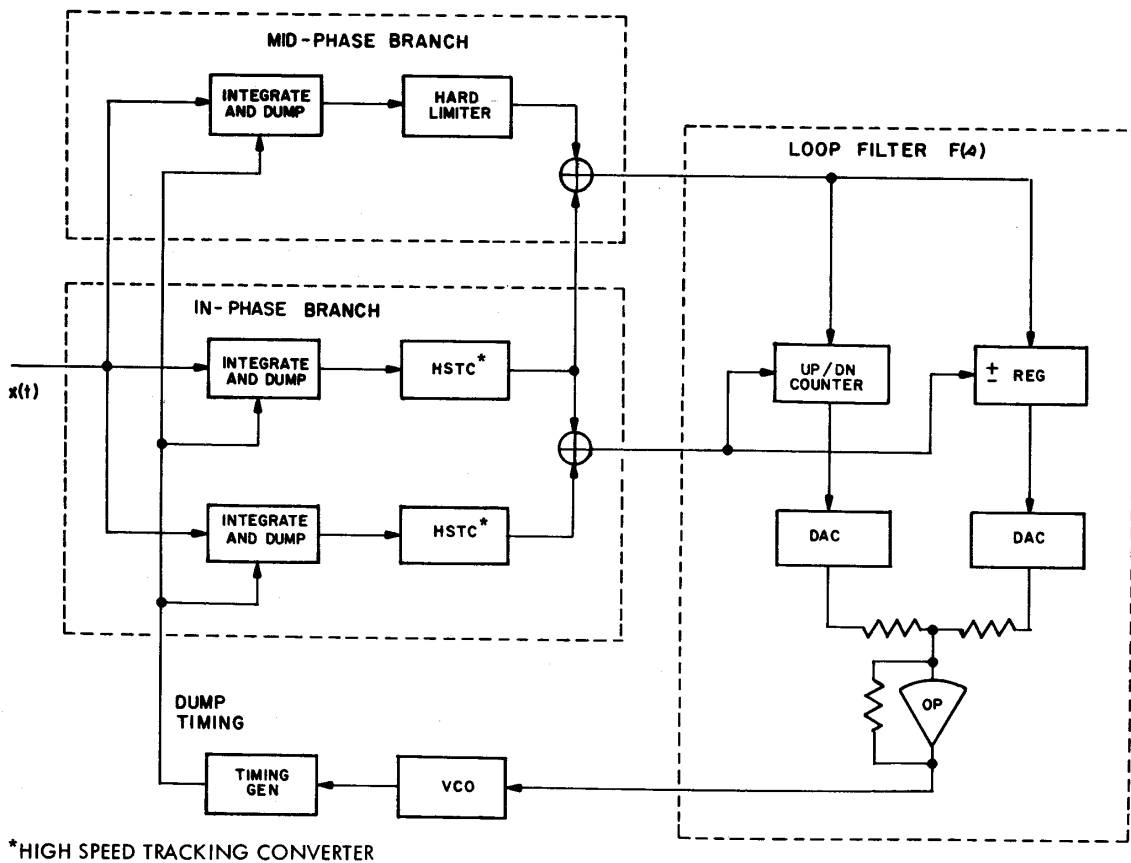


FIG. 6. FUNCTIONAL BLOCK DIAGRAM OF SYSTEM MECHANIZATION

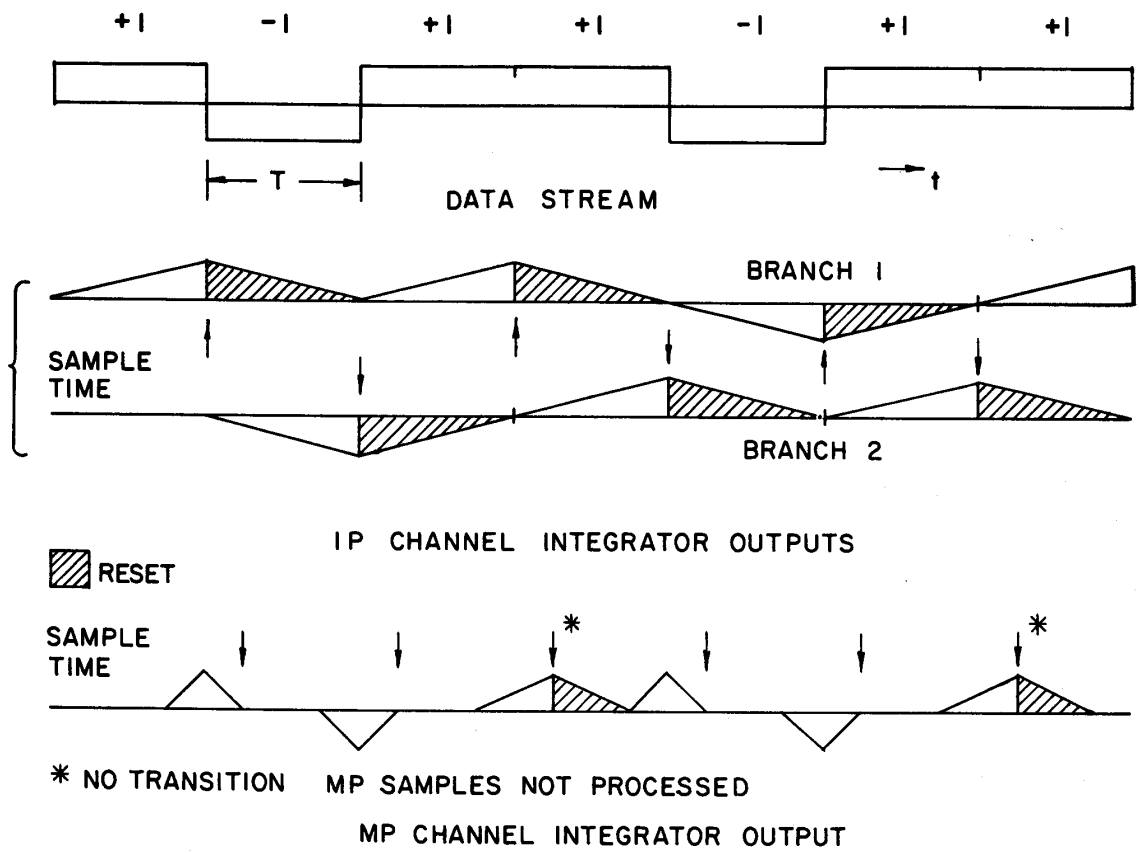


FIG. 7. SYSTEM TIMING CHART FOR $w = T/2$